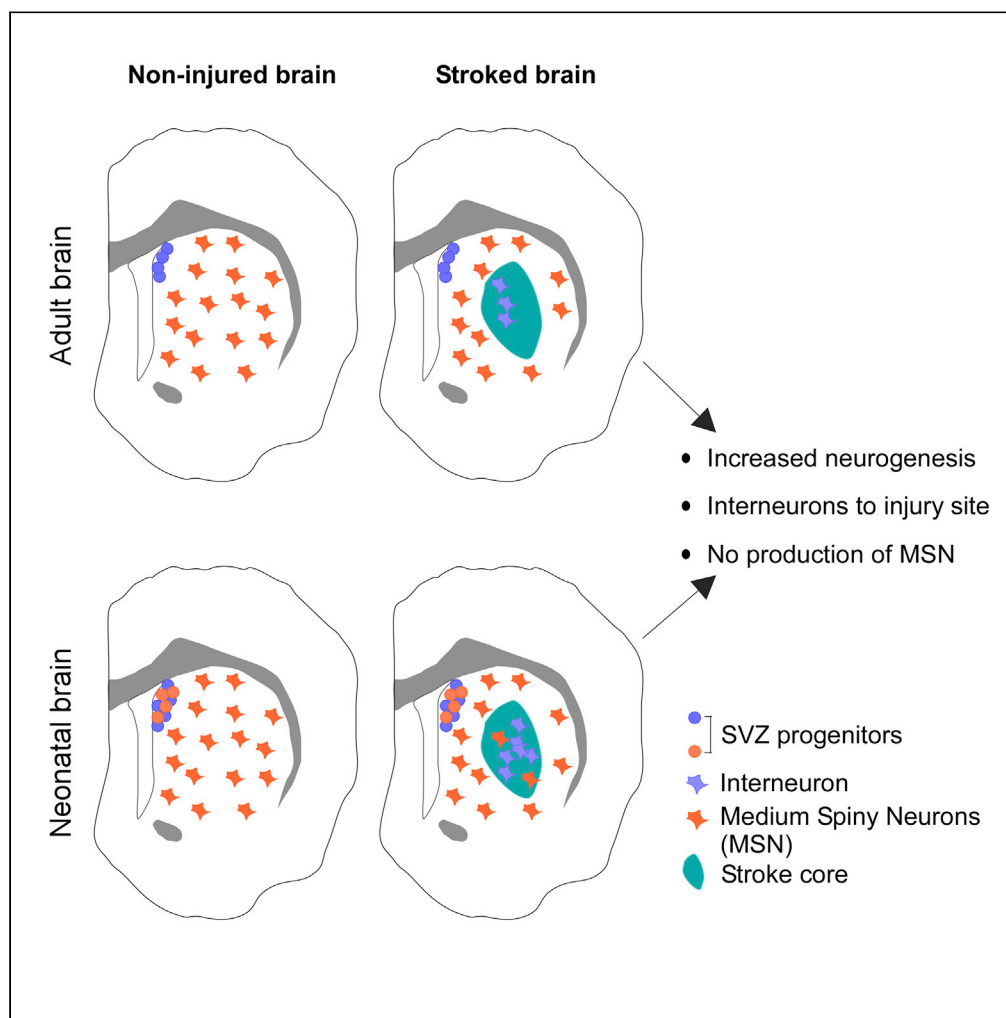


Article

Ischemic Injury Does Not Stimulate Striatal Neuron Replacement Even during Periods of Active Striatal Neurogenesis



Charlotte M. Ermine, Jordan L. Wright, Davor Stanic, Clare L. Parish, Lachlan H. Thompson

charlotte.ermine@florey.edu.au (C.M.E.)
lachlant@unimelb.edu.au (L.H.T.)

HIGHLIGHTS

Phenotyping of thousands of cells generated after striatal ischemic injury

Confirms previous reports on lack of injury-induced adult striatal neurogenesis

No “self-repair” even during active periods of neonatal striatal neurogenesis



Article

Ischemic Injury Does Not Stimulate Striatal Neuron Replacement Even during Periods of Active Striatal Neurogenesis

Charlotte M. Ermine,^{1,3,*} Jordan L. Wright,^{1,2} Davor Stanic,¹ Clare L. Parish,¹ and Lachlan H. Thompson^{1,*}

SUMMARY

Ischemic damage to the adult rodent forebrain has been widely used as a model system to study injury-induced neurogenesis, resulting in contradictory reports regarding the capacity of the postnatal brain to replace striatal projection neurons. Here we used a software-assisted, confocal approach to survey thousands of cells generated after striatal ischemic injury in rats and showed that injury fails not only to stimulate production of new striatal projection neurons in the adult brain but also to do so in the neonatal brain at early postnatal ages not previously explored. Conceptually this is significant, because it shows that even during periods of active striatal neurogenesis, injury is not a sufficient stimulus to promote replacement of these neurons. Understanding the intrinsic capacity of the postnatal brain to replace neurons in response to injury is fundamental to the development of “self-repair” therapies.

INTRODUCTION

Neurons of the central nervous system (CNS) are generated during finite windows of neurogenesis that occur as tightly orchestrated processes during embryonic development. In the mammalian CNS, all the projection neurons are produced during this developmental period; however, the production of certain types of interneurons persists throughout life in two neurogenic niches in the postnatal brain: the subventricular zone (SVZ) that lines the lateral ventricles and the subgranular zone (SGZ) adjacent to the dentate gyrus of the hippocampus (for review see [Aimone et al., 2014](#)). In both cases, stem cells within the SGZ and SVZ neurogenic regions give rise to granular interneurons, which will replenish granule cell layers in the hippocampal dentate gyrus and the olfactory bulb, respectively, as part of ongoing homeostatic processes in the healthy brain.

Whether or not these stem cells can additionally give rise to other neuronal subtypes under certain pathological circumstances, for example, in response to brain injury, remains controversial. Studies in the early 2000s reported that significant neuronal loss through damage to areas adjacent to neurogenic niches could redirect the fate of stem cell-derived neuroblasts to not only migrate to the damaged area but also differentiate into regionally appropriate neuronal subtypes including midbrain dopamine neurons ([Zhao et al., 2003](#)), CA1 pyramidal neurons ([Nakatomi et al., 2002](#)), and medium spiny projection (MSP) neurons ([Arvidsson et al., 2002](#); [Parent et al., 2002](#)). However, these findings have not been widely replicated and subsequent studies reported that projection neurons such as midbrain dopamine ([Frielingsdorf et al., 2004](#)) and medium spiny subtypes could not be generated following injury to the adult brain ([Liu et al., 2009](#)). The study by [Liu et al. \(2009\)](#) reported that injury to the striatum can indeed elicit a response from the adjacent SVZ, including an increase in proliferation of precursor cells and a redirection of the migratory path of newborn neuroblasts away from their trajectory toward the olfactory bulb and instead toward the striatal site of injury where they can differentiate into mature neurons. Interestingly, however, phenotypic analysis indicated that they did not have the capacity to change differentiation potential to adopt a striatal projection neuron identity, but rather retained their identity as olfactory bulb interneurons in an ectopic location.

Striatal MSP neurons are generated from ventricular zone (VZ) progenitor cells through a peak phase of neurogenesis during embryonic development ([Deacon et al., 1994](#); [Olsson et al., 1995](#); [van der Kooy and Fishell, 1987](#)). As development proceeds and the embryonic VZ transitions to the postnatal SVZ, the differentiation potential of VZ stem cells progressively shifts away from producing MSP neurons in favor

¹The Florey Institute for Neuroscience and Mental Health, The University of Melbourne, Parkville, VIC 3052, Australia

²Present address: Wolfson Institute for Biomedical Research, University College London, Gower Street, London WC1E 6BT, UK

³Lead Contact

*Correspondence: charlotte.ermine@florey.edu.au (C.M.E.), lachlant@unimelb.edu.au (L.H.T.)

<https://doi.org/10.1016/j.isci.2020.101175>



of the olfactory bulb interneurons that continue to be generated throughout adult life (Luskin, 1993; Alvarez-Buylla and Garcia-Verdugo, 2002). Recently we reported that the tail end of the neurogenic program for production of MSPs persists into the early neonatal period, such that SVZ cells that have shifted predominantly to the generation of olfactory bulb interneurons will also continue to contribute MSP neurons to the striatum over the first postnatal week (Wright et al., 2013). This led us to hypothesize that injury-induced regeneration of striatal projection neurons may be most likely during this early postnatal period, when proliferating SVZ precursors remain competent for production of MSPs.

To test this, we compared the phenotype of newborn neurons in the neonatal and adult rat striatum following an ischemic striatal injury causing widespread loss of striatal MSPs. A combination of automated cell counting and manual inspection of orthogonal reconstructions to unambiguously assess co-localization of markers of cell phenotype allowed us to characterize thousands of newborn cells with respect to neuronal differentiation properties after injury to neonatal or adult striatum, respectively. The results suggest that striatal injury does not stimulate striatal neuron replacement, even during periods of active striatal neurogenesis.

RESULTS

Ischemic Damage to the Adult Striatum Induces Cellular Proliferation and Neurogenesis

Injection of the vasoconstrictor ET-1 produced an ischemic injury at the site of injection, resulting in an infarcted region characterized by loss of NeuN+ neurons throughout the dorsal head of the striatum (Figure 1A). Dividing cells were labeled by daily injection of 5-bromo-2'-deoxyuridine (BrdU) (100 mg/kg), and animals were perfused for histology 3 weeks after the final BrdU injection (4 weeks after injury). Figures 1B and 1C–1G show immunohistochemistry for BrdU, NeuN, and Darpp32 and the automated detection and digital annotation of BrdU for saline- and ET-1-treated animals, respectively, using the spot creation module in Imaris 9.0. The representative images show the significant proliferative response and accumulation of BrdU+ cells (red) in the immediate vicinity of the injured area defined by loss of NeuN+/Darpp32+ cells in ET-1-injected animals relative to saline-injected controls. The total number of BrdU+ cells was significantly greater in ET-1-injected animals compared with saline controls (saline: $98,990 \pm 13,328$ cells/mm³, ET-1: $838,600 \pm 143,989$ cells/mm³, data represent mean \pm SEM, $n = 6$ /group; p value = 0.0035) (Figure 1H). Due to loss of tissue volume following ischemia, we also represented BrdU+ cells (throughout this study) as a density of striatal tissue, which again showed a significant increase following ET-1 injection compared with saline (saline: $11,581 \pm 1,944$ cells/mm³, ET-1: $120,627 \pm 26,087$ cells/mm³, p value = 0.0085; Figure 1I).

To determine the effect of injury on striatal neurogenesis, cells co-expressing both BrdU and the mature neuronal marker NeuN were quantified in the anterior head of the striatum at an interval of 1:12 between 1.7 and 0.7 mm relative to bregma. Compared with the saline-injected animals, the total number of BrdU+/NeuN+ cells in this anterior striatum was significantly greater in ET-1-injected animals (saline: 26 ± 8 cells; ET-1: 136 ± 29 cells, mean \pm SEM, $n = 12$ /group; p value = 0.0031), as was the density of striatal BrdU+/NeuN+ cells (saline: 3 ± 0.84 cells/mm³, ET-1: 19 ± 4.19 ; p value = 0.0026) (Figures 1J and 1K). The number of BrdU+/NeuN+ cells across both groups was overall low and quite variable, with most of these cells remaining in close proximity to the rostral migratory stream (Figure 1L).

Newborn Neurons following Ischemic Injury Do Not Acquire a Medium Spiny Neuron Identity

To determine the phenotypic identity of newborn neurons residing in the striatum following ischemic injury, we first assessed co-labeling of BrdU+/NeuN+ cells for the MSP neuron marker, Darpp32. Evaluation of orthogonal reconstructions of cells acquired by confocal microscopy across 12 brains did not reveal any examples of BrdU+/NeuN+ cells that also expressed Darpp32. Interestingly however, a strikingly common occurrence was the presence of BrdU+ cells in tight apposition to Darpp32+/NeuN+ cells (Figures 2A–2J). From a top-down perspective in the x-y plane these cells often presented as triple-labeled, as seen in Figures 2A and 2F, but orthogonal inspection on the y axis showed the nuclei to be distinctly separate (Figures 2E and 2J). We also observed examples at the direct site of infarction, which initially appeared as triple-labeled; however, these were subsequently shown to auto-fluoresce across all emission wavelengths and deemed non-specific (not shown). In our experience this is a common feature of immunohistochemical analysis in areas where there is significant damage-induced necrosis and inflammation, often associated with infiltration of blood cells.

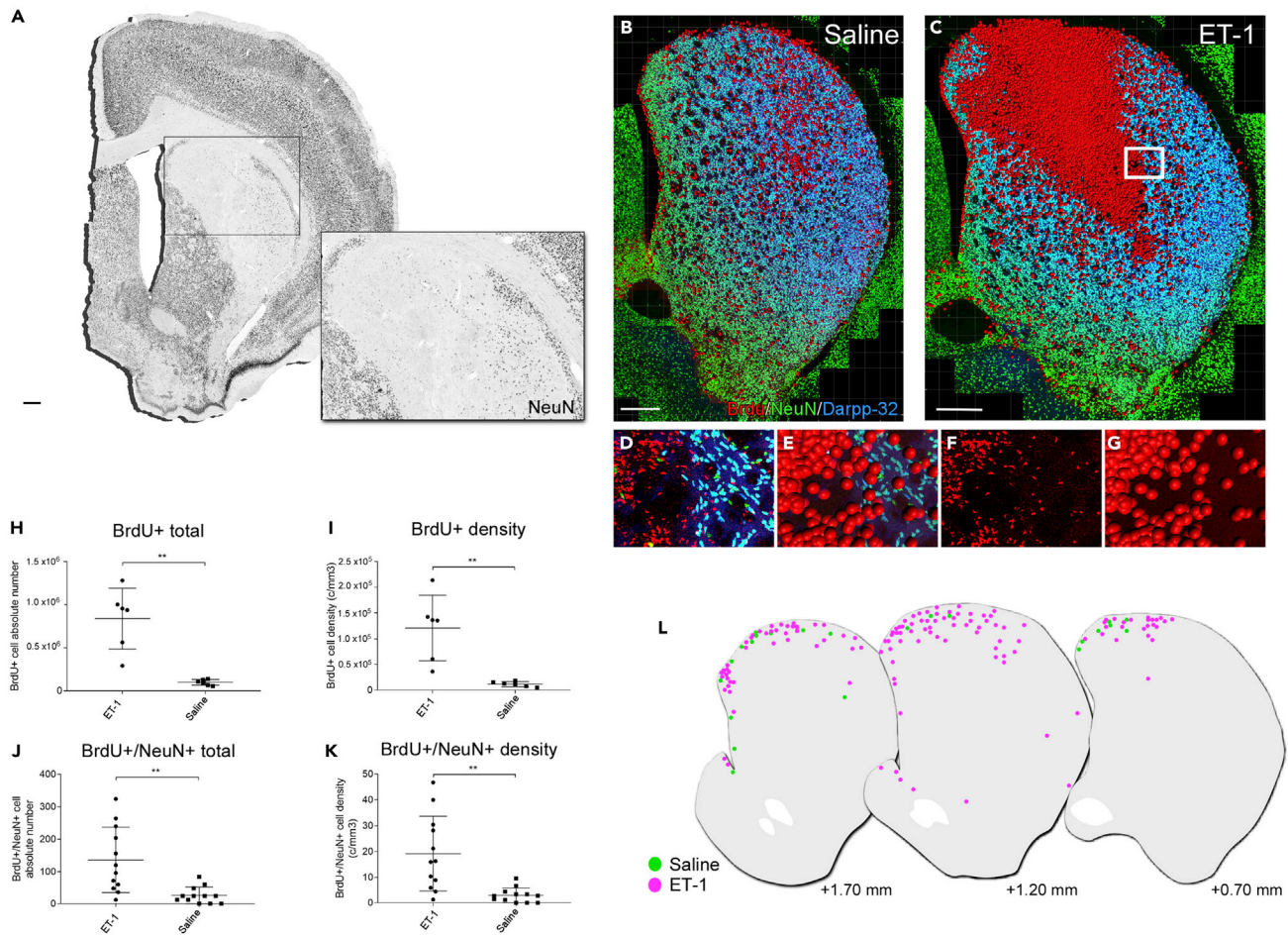


Figure 1. Proliferation and Striatal Neurogenesis Is Increased 4 Weeks after Ischemic Injury to the Adult Striatum

(A–K) (A) Immunohistochemistry for NeuN shows extensive cell loss associated with striatal ischemic injury at the level of ET-1 injection. Representative striatal sections immunohistochemically labeled for BrdU (red), NeuN (green), and Darpp-32 (blue) from saline (B) and ET-1 (C) groups illustrate the automated detection of BrdU+ cells and annotation as red spheres by Imaris software. The boxed area is represented at higher magnification without (D and F) and with annotation (E and G). The absolute number of BrdU+ cells (H) and the density of BrdU+ cells (I) are significantly increased following ET-1 injection. The absolute number of BrdU+/NeuN+ cells (J) and BrdU+/NeuN+ density (K) are significantly increased in the ET-1-injected group compared with saline control. (L) Schematic sections (+1.70 mm, +1.20 mm and +0.70 mm from bregma) illustrate the approximate location of BrdU+/NeuN+ cells cumulatively across all animals from the saline (green dots, $n = 6$) and ET-1 (pink dots, $n = 6$) groups.

Statistical analysis: (H) Welch's t test $t(5.056) = 4.169$, $p = 0.0085$, $n = 6$. (I) Welch's t test $t(5.086) = 5.115$, $p = 0.0035$, $n = 6$. (J) Welch's t test $t(12.45) = 3.650$, $p = 0.0031$, $n = 12$. (K) Welch's t test $t(11.88) = 3.794$, $p = 0.0026$, $n = 12$. ** $p < 0.01$; Error bars: Standard deviation.

Scale bars: 500 μm in (A–C).

BrdU, 5-bromo-2'-deoxyuridine.

Immunohistochemical detection of calretinin (CR; Figures 2K–2T), a calcium-binding protein found in interneurons, including those normally destined for the olfactory bulb, revealed the presence of both BrdU+/CR+/NeuN- (Figures 2K–2O) and BrdU+/CR+/NeuN+ cells (Figures 2P–2T) in sham and ET-1-treated animals. Overall, around $61 \pm 15\%$ (mean \pm SEM) of BrdU+/CR+ cells were also NeuN+. Quantification showed that the ET-1-treated animals had a significant increase in total BrdU+/CR+ cell number (saline: 54 ± 15.41 cells, ET-1: 136 ± 30.93 cells, data represent mean \pm SEM, $n = 6/\text{group}$, $p = 0.0391$) (Figure 2U) and BrdU+/CR+ cell density (saline: 5.82 ± 1.53 cells/ mm^3 , ET-1: 19.75 ± 5.39 cells/ mm^3 , $p = 0.0323$) (Figure 2V). We also observed a significant increase in BrdU+/NeuN+/CR+ cell number in the injury group (saline: 10 ± 4.8 cells; ET-1: 106 ± 35.6 cells, $p = 0.0429$) (Figure 2W) and BrdU+/NeuN+/CR+ cell density (saline: 1.20 ± 0.61 cells/ mm^3 , ET-1: 15.96 ± 5.68 cells/ mm^3 , $p = 0.0483$) (Figure 2X).

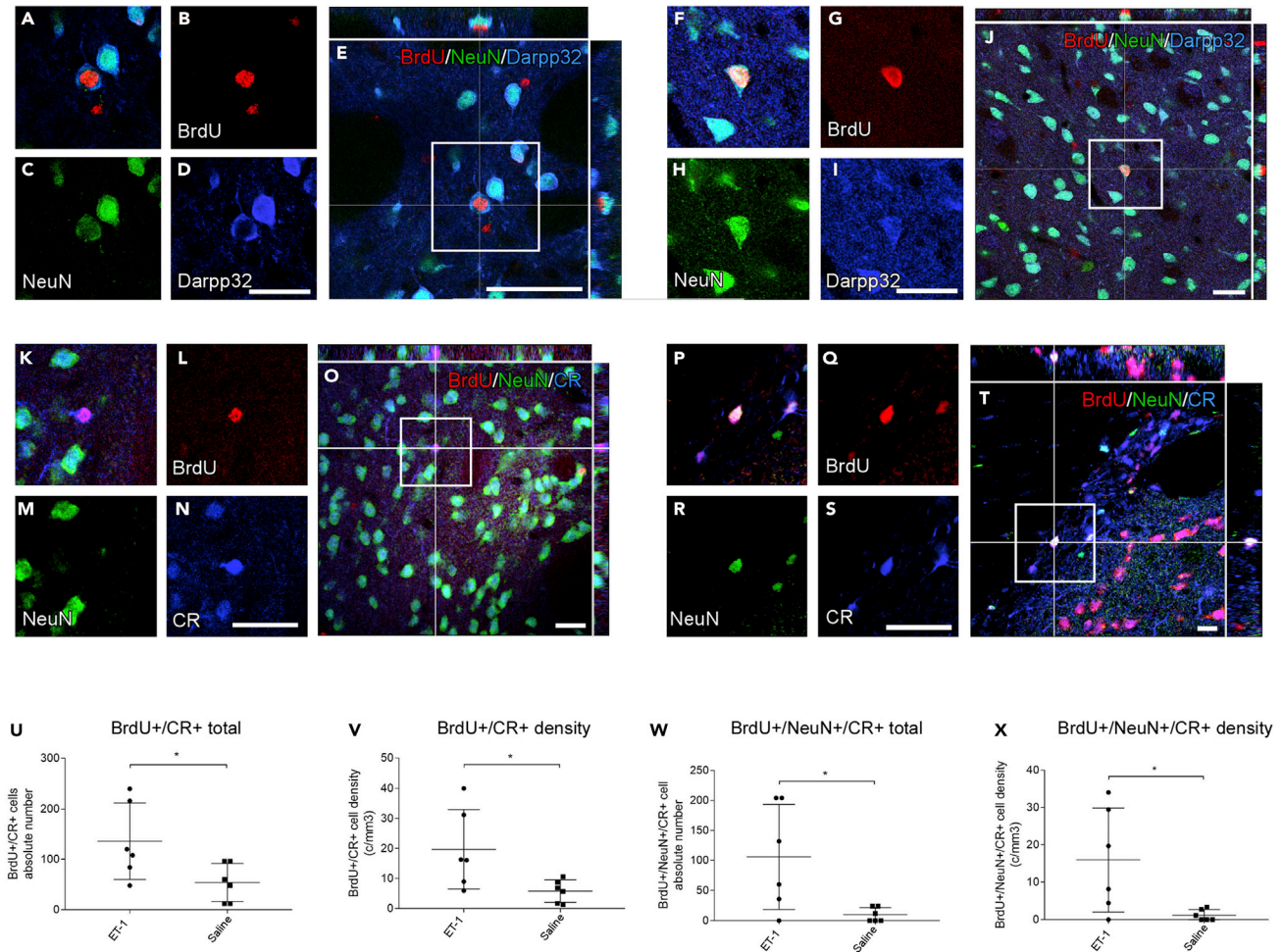


Figure 2. Ischemic Damage to the Adult Striatum Recruits Calretinin+ Interneurons but Not Medium Spiny Neurons

(A–E) and (F–J) show two examples of immunohistochemistry for BrdU (red), NeuN (green), and Darpp32 (blue) at 4 weeks after ischemia, where BrdU+ cells appear to be co-registered with Darpp32+ neurons when viewed on the x-y axes but are revealed to be adjacent and non-overlapping through orthogonal reconstruction of the z axis. Orthogonal examination of immunohistochemistry for BrdU (red), NeuN (green), and calretinin (blue) revealed the presence of new calretinin+ neurons including both NeuN+ (K–O) and NeuN- (P–T) examples. Quantification showed BrdU+/CR+ absolute number (U), BrdU+/CR+ density (V), BrdU+/NeuN+/CR+ absolute number (W), and BrdU+/NeuN+/CR+ density (X) are all significantly increased following ET-1 injection compared with saline controls.

Statistical analysis: (U) Unpaired t test $t(10) = 2.373$, $p = 0.0391$, $n = 6$. (V) Unpaired t test $t(10) = 2.484$, $p = 0.0323$, $n = 6$. (W) Welch's t test $t(5.182) = 2.668$, $p = 0.0429$, $n = 6$. (X) Welch's t test $t(5.117) = 2.581$, $p = 0.0483$, $n = 6$. * $p < 0.05$; Error bars: Standard deviation.

Scale bars: 25 μ m in (A–T).

BrdU, 5-bromo-2'-deoxyuridine; CR, calretinin; Darpp32, dopamine- and cyclic-AMP-regulated phosphoprotein of molecular weight 32,000.

Ischemic Damage to the Neonatal Striatum Does Not Induce Striatal Neurogenesis

Injection of ET-1 at postnatal day 1 produced a robust ischemic injury to the striatum and overlying cortex, manifesting at 4 weeks as hydrocephaly, significant striatal atrophy, and cortical scarring with conspicuous mushroom-like patterns reminiscent of ulegyric folding seen in cerebral palsy (Figure 3A). Immunohistochemistry for BrdU, NeuN, and Darpp32 cells showed a robust level of proliferation in both saline- (Figure 3B) and ET-1- (Figure 3C) treated neonatal animals during the first week after surgery. The absolute number of BrdU+ cells was significantly higher in the saline control group (saline: $603,348 \pm 27,413$; ET-1: $401,558 \pm 15,668$, data represent mean \pm SEM, $n = 6$ /group, $p < 0.0001$; Figure 3D); however, the ET-1 group had a significantly higher density of BrdU+ cells given the substantial striatal atrophy associated with the injury (saline: $78,685 \pm 1,806$ cells/mm³; ET-1: $110,657 \pm 2,257$ cells/mm³, $p < 0.0001$; Figure 3E).

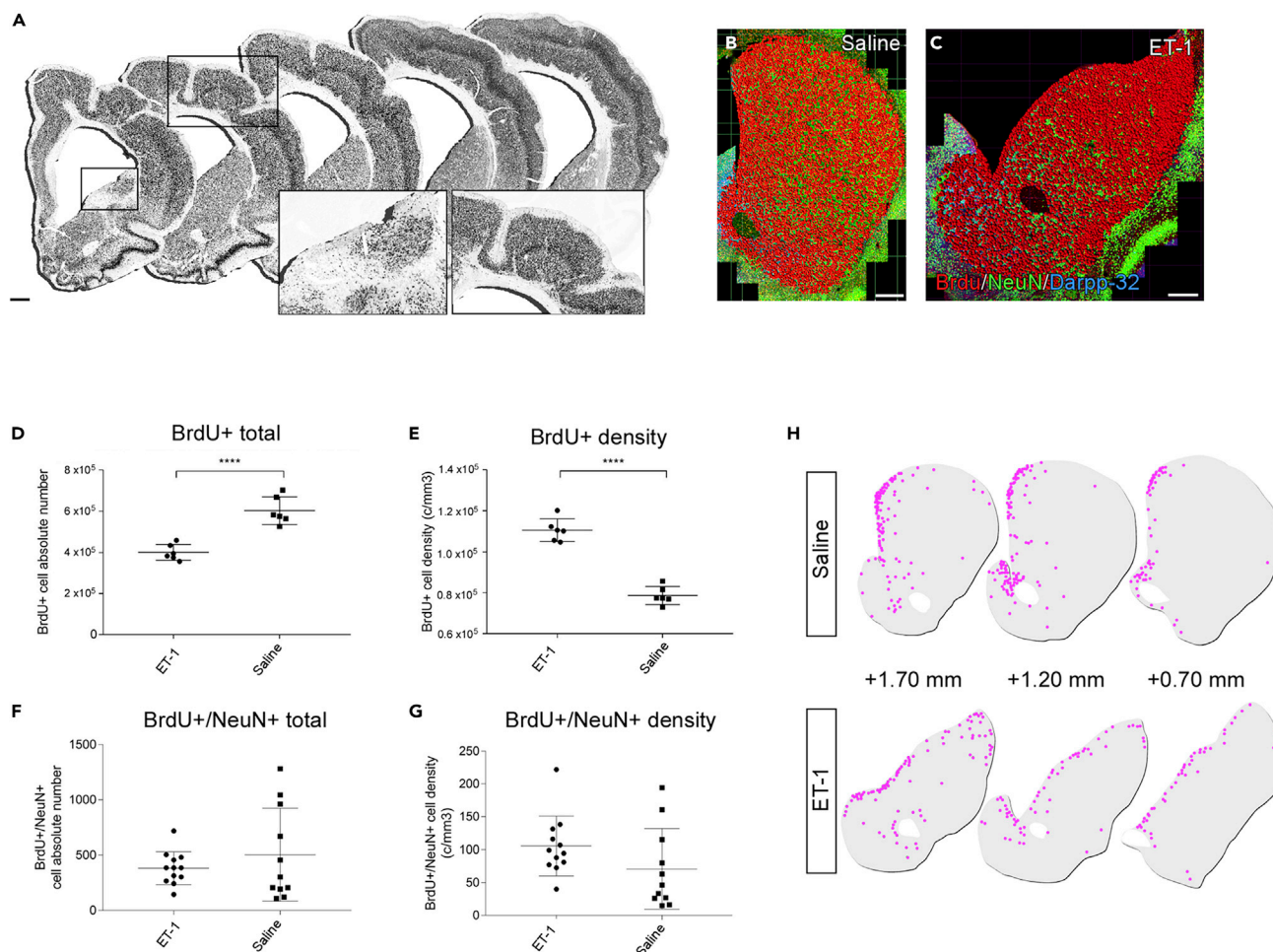


Figure 3. Ischemic Damage to the Neonatal Brain Does Not Increase Gross Striatal Neurogenesis 4 Weeks After Injury

(A–H) (A) Immunohistochemistry for NeuN in representative sections illustrates typical cortical malformation and striatal atrophy at 4 weeks following ischemic damage in the neonatal brain. Representative striatal sections immunohistochemically labeled for BrdU (red), NeuN (green), and Darpp-32 (blue) from saline (B) and ET-1 (C) groups illustrate the automated detection of BrdU+ cells and annotation as red spheres by Imaris software. Four weeks following injection of ET-1 in the neonatal striatum, the absolute number of BrdU+ cells (D) is significantly reduced compared with saline controls; however, the density of BrdU+ cells (E) is significantly increased. Double-labeling for NeuN showed that the absolute number of BrdU+/NeuN+ cells (F) and the BrdU/NeuN density (G) are not significantly different between ET-1 and saline groups 4 weeks post ischemia. (H) Schematic sections through the striatum illustrating the approximate location of BrdU+/NeuN+ cells (pink dots) cumulatively across all animals from the saline (n = 6) and ET-1 (n = 6) groups.

Statistical analysis: (D) Unpaired t test $t(10) = 6.391, p < 0.0001, n = 6$. (E) Unpaired t test $t(10) = 11.06, p < 0.0001, n = 6$. (F) Welch's t test $t(12.32) = 0.9198, p = 0.3754, n = 12$ for ET-1 and $n = 11$ for control. (G) Unpaired t test $t(21) = 1.57, p = 0.1314, n = 12$ for ET-1 and $n = 11$ for control. **** $p < 0.0001$; Error bars: Standard deviation.

Scale bars: 500 μm in (A–C).

BrdU, 5-bromo-2'-deoxyuridine.

Newborn neurons generated in the first week after saline or ET-1 injection were identified based on co-expression of BrdU and NeuN as described for the adult groups. Quantification across three striatal levels in coronal sections showed no significant difference in BrdU+/NeuN+ cells between saline- and ET-1-treated animals, either in absolute number (saline: 504 ± 127 cells, $n = 11$; ET-1: 381 ± 43 cells, $n = 12, p = 0.3754$; Figure 3F) or striatal density (saline: 70.6 ± 18.4 cells/ mm^3 ; ET-1: 105.7 ± 13.1 cells/ $\text{mm}^3, n = 12, p = 0.1314$; Figure 3G). The new BrdU+/NeuN+ neurons were found predominately in close proximity to the SVZ and rostral migratory stream (RMS) and also notably in the deeper parenchyma of the nucleus accumbens, in close proximity to the anterior commissure (Figure 3H). The pattern of distribution was similar in saline and ET-1-treated animals.

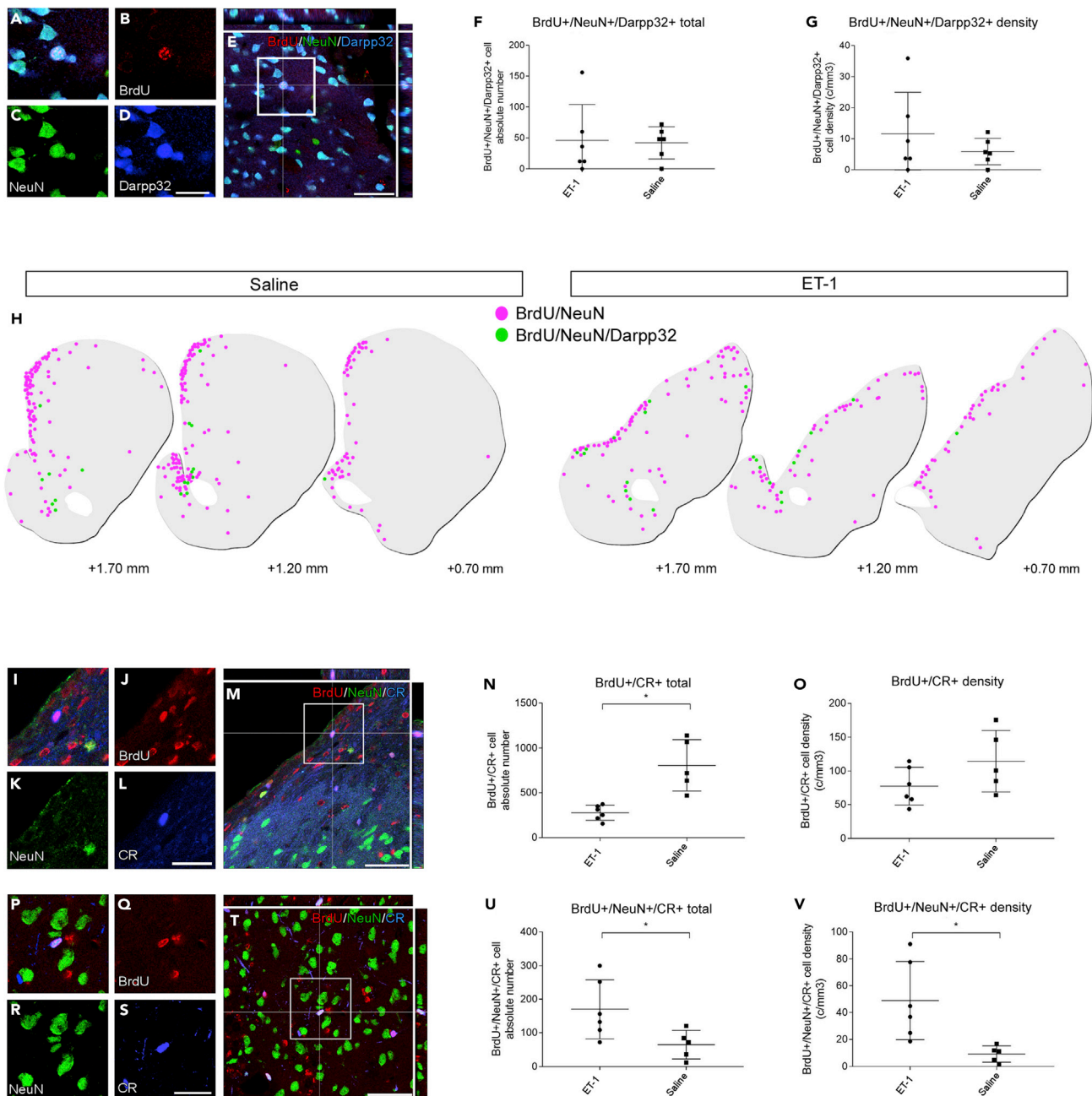


Figure 4. Neonatal Ischemia Does Not Influence the Constitutive Production of Medium Spiny Projection Neurons 4 Weeks after Injury

(A–G) (A–E) Orthogonal reconstruction of immunohistochemical labeling for BrdU (red), NeuN (green), and Darpp32 (blue) identifies that new BrdU+/NeuN+/Darpp32+ neurons are generated during the early neonatal period. The absolute numbers (F) and the densities (G) of BrdU+/NeuN+/Darpp32+ cells were not significantly different between ET-1- and saline-injected groups.

(H) Schematic sections illustrating the approximate location of BrdU+/NeuN+ cells (pink dots) and BrdU+/NeuN+/Darpp-32+ cells (green dots) cumulatively across all animals from the saline (n = 5) and ET-1 (n = 6) groups.

(I–V) (I–M) Immunohistochemical labeling showed that a population of BrdU+/CR+ cells (red and blue, respectively) that did not express NeuN (green) was actively generated in the neonatal brain. The absolute number of BrdU+/CR+/NeuN- cells was significantly greater in the ET-1 group compared with saline controls (N) but the density was unchanged (O). A second population of newly generated BrdU+/CR+ that did express NeuN could also be identified in the neonatal brain (P–T). The absolute numbers (U) of BrdU+/NeuN+/CR+ cells and the densities (V) were not significantly different between the ET-1 and saline control groups at 4 weeks.

Statistical analysis: (F) Unpaired t test $t(10) = 0.1541$, $p = 0.8806$, $n = 6$. (G) Welch's t test $t(6.009) = 1.001$, $p = 0.3554$, $n = 6$. (N) Welch's t test $t(4.554) = 3.989$, $p = 0.0126$, $n = 5$ for sham and $n = 6$ for ET-1. (O) Unpaired t test $t(9) = 1.653$, $p = 0.1327$, $n = 5$ for sham and $n = 6$ for ET-1. (U) Unpaired t test $t(9) = 2.435$,

Figure 4. Continued

$p = 0.0376$, $n = 5$ for sham and $n = 6$ for ET-1. (V) Welch's t test $t(5.507) = 3.246$, $p = 0.0198$, $n = 5$ for sham and $n = 6$ for ET-1. * $p < 0.05$; Error bars: Standard deviation.

Scale bars: 25 μm in (A–E) and 50 μm in (I–M) and (P–T).

BrdU, 5-bromo-2'-deoxyuridine; Darpp32, dopamine- and cyclic-AMP-regulated phosphoprotein of molecular weight 32,000; CR, calretinin.

The Production of Darpp32+ Striatal Neurons in the Early Neonatal Period Is Not Affected by Striatal Injury

New Darpp32+ striatal projection neurons generated in the first week after ET-1 or control saline injection into the neonatal striatum were identified by validation of co-expression of BrdU, NeuN, and Darpp32+ in orthogonal re-constructions of confocal images (Figures 4A–4E). Quantification did not reveal any difference between ET-1-treated and saline-animals in either the absolute number (saline: 42 ± 11 cells; ET-1: 46 ± 24 cells, mean \pm SEM, $n = 6$ /group, $p = 0.8806$; Figure 4F) or density (saline: 5.91 ± 1.74 cells/ mm^3 ; ET-1: 11.63 ± 5.44 cells/ mm^3 , $n = 6$ /group, $p = 0.3554$; Figure 4G) of BrdU+/NeuN+/Darpp32+ cell density in the striatum 4 weeks after surgery. In both groups, the BrdU+/NeuN+/Darpp32+ cells were found close to the SVZ and in the nucleus accumbens (Figure 4H).

Analysis of immunohistochemistry for CR showed the presence of BrdU+/CR+/NeuN- cells (Figures 4I–4M) in both ET-1- and saline-injected animals. Quantification at 4 weeks showed that there was significantly more BrdU+/CR+ cells in the control group compared with the ET-1-treated animals (saline: 806.4 ± 128.6 cells, $n = 5$; ET-1: 276 ± 33.8 cells, $n = 6$, $p = 0.0126$; Figure 4N), although there was no difference between the two groups when represented as striatal density (saline: 114.4 ± 20.4 cells/ mm^3 ; ET-1: 77.4 ± 11.5 cells/ mm^3 , $n = 6$, $p = 0.1327$; Figure 4O). We also identified BrdU+/CR+/NeuN+ cells (Figures 4P–4T), with quantification showing that ET-1 treatment led to a significant increase in absolute number (saline: 64.8 ± 18.8 cells, $n = 5$; ET-1: 170 ± 35.9 cells, $n = 6$, $p = 0.0376$; Figure 4U) and striatal density (saline: 9.27 ± 2.70 cells/ mm^3 , $n = 5$; ET-1: mean \pm SEM = 48.97 ± 11.93 cells/ mm^3 , $n = 6$, $p = 0.0198$; Figure 4V).

To assess whether neonatal ischemic damage affected striatal neurogenesis that manifested over a more protracted timeline following the injury, we examined the ET-1 and saline groups with a longer 12-week chase period following the 1-week BrdU pulse. The ET-1-induced ischemic pathology appeared similar to the assessment at 4 weeks, with hydrocephaly, striatal atrophy, and glial scarring in the striatum and overlying cortex (Figure 5A). Immunohistochemical analysis showed robust labeling of BrdU+ cells in both the saline control (Figure 5B) and ET-1 (Figure 5C) groups. The number of BrdU+ cells was significantly reduced in the ET-1 group (saline: $37,891 \pm 3,249$ cells; ET-1: $40,363 \pm 4,070$ cells, mean \pm SEM, $n = 5$ /group, $p = 0.6477$; Figure 5D), although not when represented as striatal density given the substantial atrophy in the ET-1 group (control: $347,863 \pm 25,334$ cells/ mm^3 ; ET-1: $216,310 \pm 32,005$ cells/ mm^3 , $p = 0.0122$; Figure 5E). The number of new, BrdU+/NeuN+ neurons generated in the first week after saline or ET-1 injection and surviving to 12 weeks was also lower in ET-1 animals, although not significantly (saline: mean \pm SEM = 696 ± 84.21 cells, $n = 5$; ET-1: mean \pm SEM = 831 ± 95.19 cells, $n = 5$, $p = 0.3214$; Figure 5F) and the striatal density was similar in the ET-1 and control groups (saline: mean \pm SEM = $6,386 \pm 728.96$ cells/ mm^3 , $n = 5$; ET-1: mean \pm SEM = $4,418 \pm 663.30$ cells/ mm^3 , $n = 5$, $p = 0.0809$; Figure 5G). The topographical distribution of new neurons was similar to that observed at 4 weeks, predominately close to the SVZ and in the nucleus accumbens (Figure 5H), although clearly in greater numbers.

As per the 4-week groups, BrdU+/NeuN+ cells present at 12 weeks were assessed for co-expression of phenotypic markers Darpp32 (Figures 6A–6H) and CR (Figures 6I–6V). Quantification showed that there was no significant difference in the number of BrdU+/NeuN+/Darpp32+ neurons in ET-1-injured or saline control groups (saline: $3,403 \pm 507$ cells; ET-1: $2,095 \pm 446$ cells, mean \pm SEM, $n = 5$ /group, $p = 0.089$; Figure 6F) or their striatal density (saline: 370.2 ± 56.6 cells/ mm^3 ; ET-1: 388.1 ± 66.9 cells/ mm^3 , $p = 0.8425$; Figure 6G). The distribution of BrdU+/NeuN+/Darpp32+ neurons at 12 weeks (Figure 6H) was similar to the pattern observed at 4 weeks, although there were clearly greater numbers at 12 weeks and a more greater representation in the deeper striatal parenchyma, more distal to the SVZ.

Similarly, neither was there significant difference in the absolute number (saline: mean \pm SEM = 38.90 ± 4.46 cells/ mm^3 , $n = 5$; ET-1: mean \pm SEM = 65.66 ± 25.11 cells/ mm^3 , $n = 5$, $p = 0.3501$; Figure 6N) or density (saline: mean \pm SEM = 357.6 ± 36.67 cells, $n = 5$; ET-1: mean \pm SEM = 319.2 ± 99.58 cells, $n = 5$,

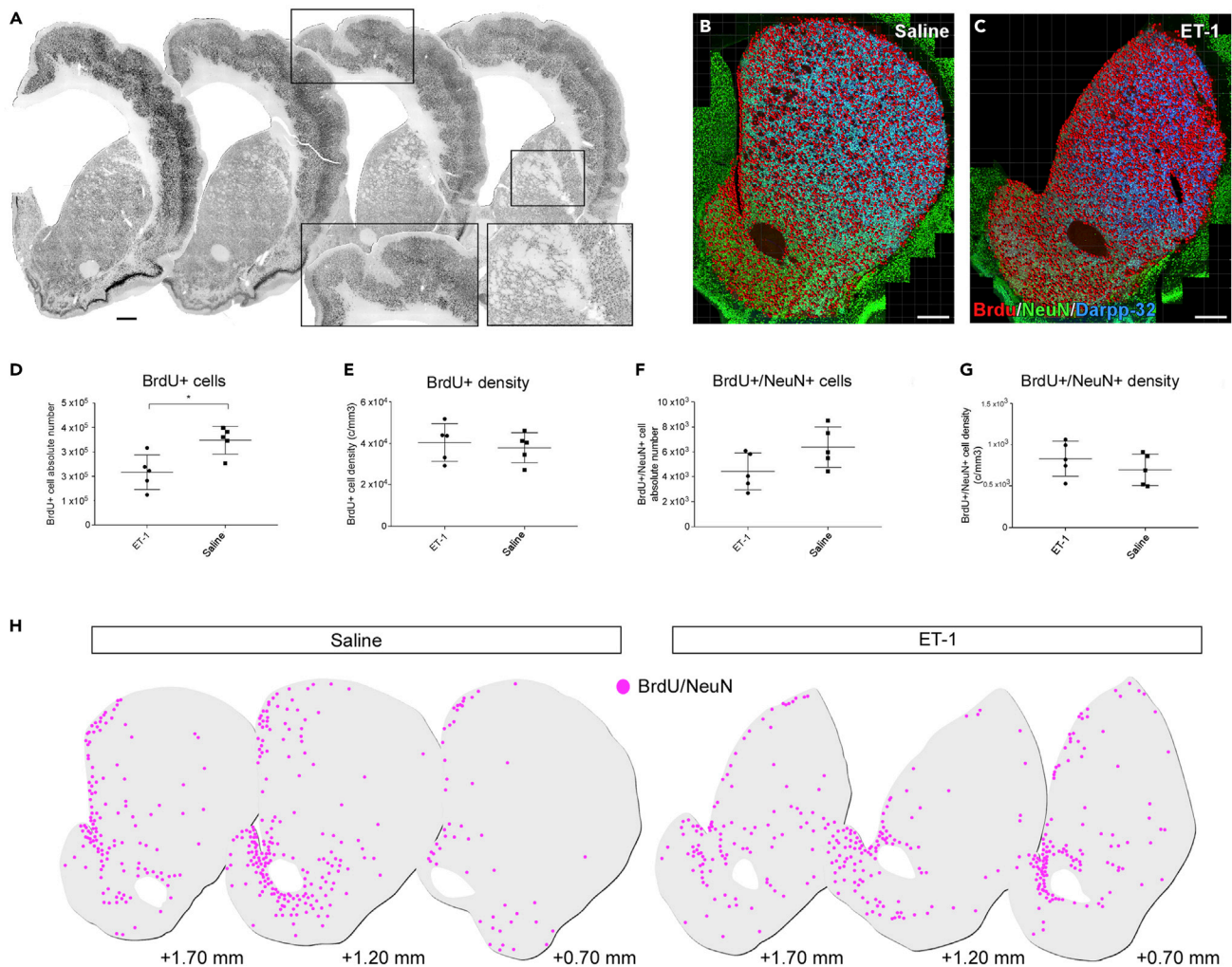


Figure 5. Ischemic Damage to the Neonatal Brain Does Not Increase Gross Striatal Neurogenesis 12 Weeks after Injury

(A–G) (A) Immunohistochemistry for NeuN in representative sections illustrates typical cortical malformation and striatal atrophy at 12 weeks following ischemic damage in the neonatal brain. Representative striatal sections immunohistochemically labeled for BrdU (red), NeuN (green), and Darpp-32 (blue) from saline (B) and ET-1 (C) groups illustrate the automated detection of BrdU+ cells and annotation as red spheres by Imaris software. Twelve weeks following injection of ET-1 in the neonatal striatum, the absolute number of BrdU+ cells (D) is significantly reduced compared with saline controls; however, the density of BrdU+ cells (E) is unchanged. Double-labeling for NeuN showed that the absolute number of BrdU+/NeuN+ cells (F) and the BrdU/NeuN density (G) are not significantly different between ET-1 and saline groups 12 weeks post-ischemia. (H) Schematic sections through the striatum illustrate the approximate location of BrdU+/NeuN+ cells (pink dots) cumulatively across all animals from the saline (n = 6) and ET-1 (n = 6) groups. Statistical analysis: (D) Unpaired t test $t(8) = 3.223$, $p = 0.0122$, $n = 5$. (E) Unpaired t test $t(8) = 0.4747$, $p = 0.6477$, $n = 5$. (F) Unpaired t test $t(8) = 1.997$, $p = 0.0809$, $n = 5$. (G) Unpaired t test $t(8) = 1.057$, $p = 0.3214$, $n = 5$. * $p < 0.05$; Error bars: Standard deviation.

Scale bars: 500 μm in (B and C).

BrdU, 5-bromo-2'-deoxyuridine.

$p = 0.7268$; Figure 6O) of BrdU+/CR+/NeuN- cells nor was there a significant difference in the number (control: mean \pm SEM = 170.4 ± 24.71 cells, $n = 5$; ET-1: mean \pm SEM = 177.6 ± 55.43 cells, $n = 5$, $p = 0.9085$; Figure 6U) or density (control: mean \pm SEM = 18.41 ± 2.69 cells/ mm^3 , $n = 5$; ET-1: mean \pm SEM = 36.32 ± 13.37 cells/ mm^3 , $n = 5$, $p = 0.2545$; Figure 6V) of BrdU+/CR+/NeuN+ cells.

DISCUSSION

Research on adult neurogenesis in the mammalian brain has often been controversial, ranging from recent lack of consensus as to whether it continues at all in the human brain after the early postnatal period (Lucassen et al., 2019) to the present topic regarding the capacity of injury to stimulate regeneration of

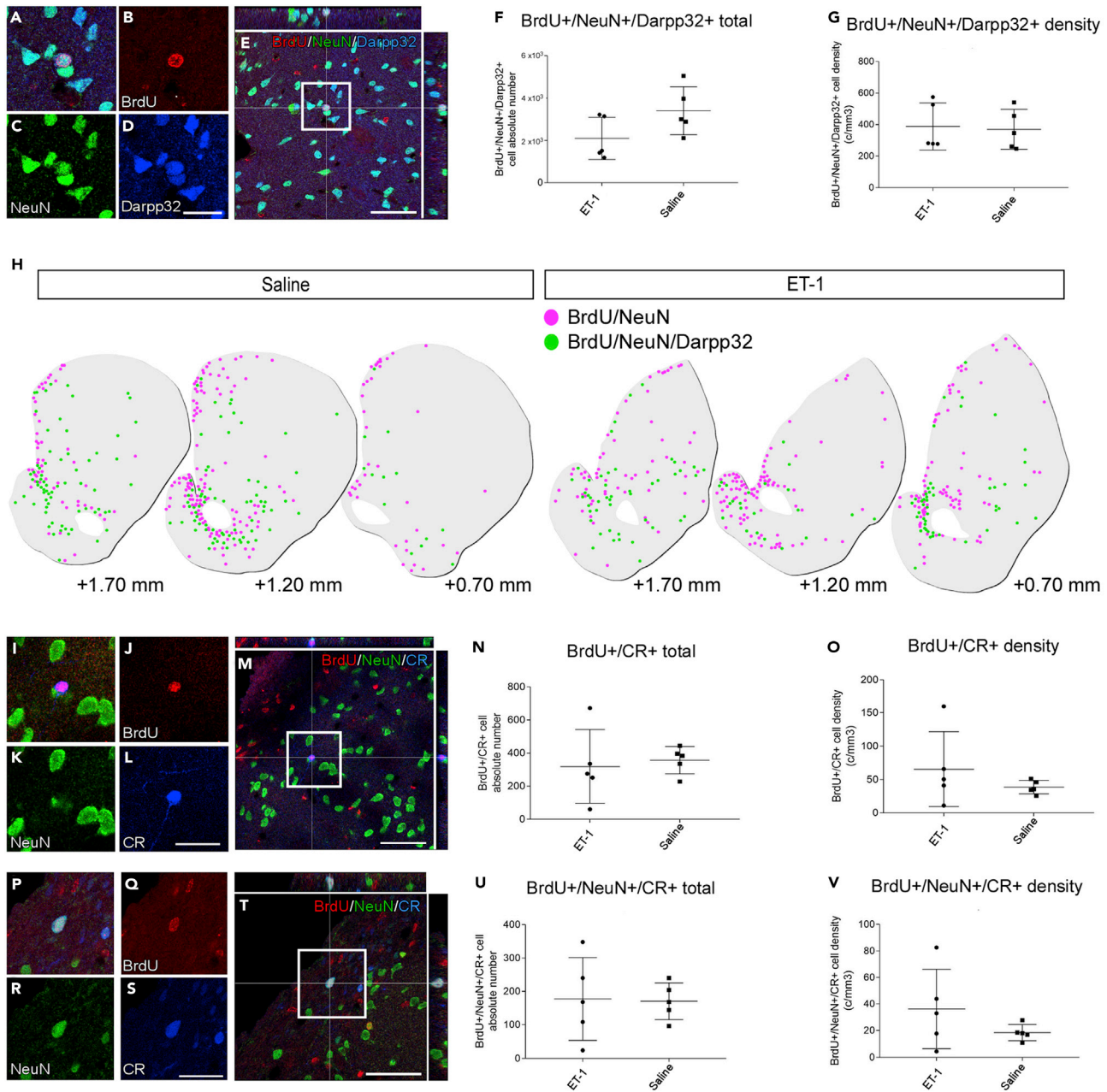


Figure 6. Neonatal Ischemia Does Not Influence the Constitutive Production of Medium Spiny Projection Neurons 12 Weeks after Injury

(A–G) (A–E) Orthogonal reconstruction of immunohistochemical labeling for BrdU (red), NeuN (green), and Darpp32 (blue) identify new BrdU+/NeuN+/Darpp32+ neurons generated during the early neonatal period. The absolute numbers (F) and the densities (G) of BrdU+/NeuN+/Darpp32+ cells were not significantly different between ET-1- and saline-injected groups.

(H) Schematic sections (+1.70 mm, +1.20 mm, and +0.70 mm from bregma) illustrate the approximate location of BrdU+/NeuN+ cells (pink dots) and BrdU+/NeuN+/Darpp32+ cells (green dots) cumulatively across all animals from the saline (n = 5) and ET-1 (n = 5) groups.

(I–V) (I–M) Immunohistochemical labeling showed a population of BrdU+/CR+ cells (red and blue, respectively) that did not express NeuN (green) was actively generated in the neonatal brain. Both the absolute number (N) and density (O) of BrdU+/CR+/NeuN- cells was not significantly different between ET-1 and saline control groups. A second population of newly generated BrdU+/CR+ that did express NeuN could also be identified in the neonatal brain (P–T). The absolute number (U) of BrdU+/NeuN+/CR+ cells and the average density (V) were not significantly different between the ET-1 and saline control groups at 12 weeks.

Statistical analysis: (F) Unpaired t test $t(8) = 1.936$, $p = 0.0888$, $n = 5$. (G) Unpaired t test $t(8) = 0.2053$, $p = 0.8425$, $n = 5$. (N) Unpaired t test $t(8) = 0.3619$, $p = 0.7268$, $n = 5$. (O) Welch's t test $t(4.252) = 1.049$, $p = 0.3501$, $n = 5$. (U) Unpaired t test $t(8) = 0.1186$, $p = 0.9085$, $n = 5$. (V) Welch's t test $t(4.322) = 1.313$, $p = 0.2545$, $n = 5$. Error bars: Standard deviation.

Scale bars: 25 μ m in (A–E), (I–M), and (P–T).

BrdU, 5-bromo-2'-deoxyuridine; Darpp32, dopamine- and cyclic-AMP-regulated phosphoprotein of molecular weight 32,000; CR, calretinin.

neuronal subtypes that are normally only produced during embryonic development. Here we have used an approach combining software-automated identification of BrdU+ cells co-labeled for markers of phenotypic identity followed by manual verification in orthogonal reconstructions, to screen thousands of newborn cells generated following striatal ischemia in neonatal or adult rats. The results indicate that loss of striatal projection neurons does not trigger their replacement through a neurogenic “self-repair” process.

The widespread loss of striatal neurons following injection of ET-1 into the adult forebrain is consistent with the pattern of ischemic damage we (Ermine et al., 2019; Somaia et al., 2017) and others (Gilmour et al., 2004) have previously reported and shown to be associated with a deficit in motor function that is stable over months. The robust proliferative response to injury, shown as a significant increase in BrdU+ cells relative to saline-treated controls, is a well-described response to acute brain injuries (Cavanagh, 1970; Nait-Oumesmar et al., 1999; Wright et al., 2016) including those arising from ischemic damage (Arvidsson et al., 2002; Liu et al., 2009; Parent et al., 2002). Automated analysis of whole striatal sections captured as three-dimensional tissue volumes using confocal microscopy and Imaris 9.1 allowed us to identify and examine a total of ~420,000 BrdU+ cells across 6 ET-1-treated animals and ~50,000 BrdU-labeled cells across 6 animals in the saline control group. The BrdU dosing regimen of 50 mg/kg at 12-h intervals has previously been shown to capture all dividing cells during the pulse period (Arvidsson et al., 2002) and likely represented the overwhelming majority of cells born in the first week after injury.

The significant increase in newborn cells in the adult striatum adopting a neuronal (BrdU+/NeuN+) identity after ischemic injury is consistent with many previous studies reporting striatal neurogenesis in response to stroke (Arvidsson et al., 2002; Parent et al., 2002; Plane et al., 2008; Teramoto et al., 2003) and appears to be a broadly conserved physiological response to acute striatal injury with similar observations following excitotoxic lesions (Collin et al., 2005; Wright et al., 2016) or trauma (Chen et al., 2003). Whether these new neurons can contribute to recovery remains an open question. Although there have been some correlative studies on the magnitude of neurogenesis and post-stroke recovery (for review see Marlier et al., 2015), there is no clear causal link. New neurons accounted for only a small fraction of the proliferative response to injury to the adult striatum, with NeuN+/BrdU+ cells representing only ~0.00014% of all BrdU+ cells. The distribution of these cells located close to the SVZ but also dorsally, adjacent to the RMS, suggests that in addition to proliferation and migration of SVZ cells, neuroblasts already en route to the olfactory bulb via the RMS can divert ventrally into the striatal parenchyma. It is unknown whether this affects the normal contribution of these cells to the olfactory bulb, and this may be worth investigating in future studies. Although we did not look beyond neuronal phenotype to characterize the remaining BrdU+ cells in the present study, we (Irvin et al., 2008; Wright et al., 2016) and others (Amat et al., 1996; Marty et al., 1991) have previously reported that many of these are locally dividing glial cells in the striatal parenchyma, including up to 40% microglia.

Although no newborn neurons generated after ischemia in adult rats were found to co-label with the striatal projection neuron marker Darpp32, many were found to be closely apposed to Darpp32+ neurons and some were also found to label non-specifically at the site of infarction. There were, however, many examples of new BrdU+ neurons that co-expressed CR, consistent with an interneuron identity. These observations are in line with those from studies where we (Wright et al., 2016) and others (Liu et al., 2009) have previously reported a lack of neuronal differentiation into striatal projection neurons following injury and supports the idea that striatal damage can redirect olfactory-bound neuroblasts from the SVZ and RMS toward the site of damage, but without changing their intrinsic capacity for differentiation as granular layer interneurons.

This led us to consider that replacement of striatal projection neurons following damage may depend on the presence of progenitors competent for production of these neurons at the time of injury. Although the bulk of MSN production in the rodent brain occurs embryonically, with a peak production between embryonic days 12–17 (Deacon et al., 1994; Olsson et al., 1995; van der Kooy and Fishell, 1987), the tail end of this neurogenic program extends into the early postnatal period (Wright et al., 2013). Injection of ET-1 into the striatum in neonatal rats produced an ischemic injury manifesting at 4 and 12 weeks as striatal atrophy with concomitant hydrocephaly as well as malformation of the overlying cortex. We have recently shown that this model captures various elements relevant for pre-term brain injury leading to cerebral palsy, such as white matter damage and motor deficit (Wright et al., 2018).

To assess the impact of striatal injury on neurogenesis during this early postnatal period, birth-dating was performed over the first week after ET-1 injection and histology was performed at both 4 and 12 weeks to allow for the possibility of a delayed or protracted response. Large numbers of BrdU+ cells were seen in saline-injected control animals, reflecting the high rate of proliferation in the neonatal brain. Although the absolute number of BrdU+ cells was in fact greater in saline compared with ET-1-treated animals this likely reflects the smaller striatal volume due to ET-1-induced atrophy. In support of this, when represented as a density, BrdU+ cell numbers were greater in the ET-1 group at 4 weeks. Immunohistochemical analysis showed the presence of BrdU+/NeuN+ neurons in all animals and included both Darpp-32+ and CR+ subtypes as we have previously reported in naive animals (Wright et al., 2013). In both saline- and ET-1-treated animals, these new neurons were distributed predominately around the SVZ and RMS, but unlike the adult groups, they were also distributed throughout the deeper striatal parenchyma, particularly in and around the anterior commissure. This is in line with previous studies showing the persistence of striatal neurogenesis in the uninjured postnatal mammalian brain, including production of GABAergic interneurons (De Marchis et al., 2004; Inta et al., 2008; Sanai et al., 2011) and more recently, striatal projection neurons (Wright et al., 2013), which declines sharply in the first week after birth.

The number of new striatal neurons was not significantly affected by neonatal ischemic injury when measured at 4 or 12 weeks and, importantly, this was also the case when looking at the subset of DARPP32+ neurons. Thus, even in the early neonatal period when there are actively dividing SVZ precursors producing striatal projection neurons, striatal ischemia does not stimulate the additional recruitment of these neurons to replace those lost to the injury. The very early age at which the injury occurred in the present study (P1) is significant because it corresponds to an active phase of production of DARPP32+, which we have previously shown declines sharply by P5 (Wright et al., 2013). Similar studies of hypoxic-ischemic damage in the neonatal period have also reported a lack of new DARPP32+ neurons, but have been performed at ages beyond P5 and after a perceptible period of neurogenesis for this cell types (Yang et al., 2008). Not only the number of Darpp32+/BrdU+ neurons but also their topographical distribution remains remarkably consistent across the control and ET-1 groups, further supporting the conclusion that the ongoing neurogenic program is essentially impervious to injury. The increase in CR+/NeuN+/BrdU+ cells at 4 weeks suggests a redirection of olfactory-bound neuroblasts in a manner similar to that observed after injury to the adult brain. This was no longer evident at 12 weeks, which may indicate a lack of survival of these neurons, perhaps due to the ectopic location or an inflammatory environment post-injury.

In summary, we report here that ischemic striatal injury resulting in substantial loss of striatal projection neurons does not stimulate the replacement of these cells in the adult or neonatal brain. Although it is clear from the present findings and previous reports that striatal injury can result in the appearance of new striatal neurons, on balance it appears this represents a re-direction of constitutively generated neuroblasts from the SVZ or RMS to the site of injury and not the generation of Darpp32+ striatal projection neurons. Importantly, the present study also shows that injury does not promote striatal neuron replacement even during periods of active birth of striatal projection neurons. Thus, injury itself appears to be insufficient as an extrinsic signaling pathway for regulation of otherwise highly conserved neurogenic programs. Although self-repair strategies remain a fascinating prospect for restorative neurology, successful replacement of projection neurons will likely require additional signaling components including cell-intrinsic determinants of differentiation outcome. Recent reports of forced differentiation to specific neuronal phenotypes through cell-intrinsic over-expression of neurogenic transcription factors *in vivo* (Li and Chen, 2016) suggest this may also be an interesting approach for facilitating cellular replacement after stroke.

Limitations of the Study

- We did not include additional phenotypic markers of immature striatal projection phenotype. Although DARPP32 is regarded as definitive for mature identity, we cannot exclude an initial neurogenic response to produce striatal projection progenitors that ailed to survive.
- This study does not consider injury-induced neurogenesis in other areas of the brain that can be affected by this model of stroke, for example, in the hippocampus or cortex. Thus conclusions on a general lack of capacity for "self-repair" should be limited to striatal projection neurons.

Resource Availability

Lead Contact

Charlotte Ermine, charlotte.ermine@florey.edu.au.

Materials Availability

Requests for further information and reagents should be directed to and will be fulfilled by charlotte.ermine@florey.edu.au or lachlant@unimelb.edu.au.

Data and Code Availability

Requests for further information or biological data should be directed to and will be fulfilled by charlotte.ermine@florey.edu.au or lachlant@unimelb.edu.au.

METHODS

All methods can be found in the accompanying [Transparent Methods supplemental file](#).

SUPPLEMENTAL INFORMATION

Supplemental Information can be found online at <https://doi.org/10.1016/j.isci.2020.101175>.

ACKNOWLEDGMENTS

The authors thank Mong Tien for expert technical assistance in the tissue preparation and immunohistochemical procedures. C.L.P. is an NHMRC Senior Research Fellow. This work was supported NHMRC project grant 1130734. The Florey Institute of Neuroscience and Mental Health acknowledges the strong support from the Victorian Government and in particular the funding from the Operational Infrastructure Support Grant.

AUTHOR CONTRIBUTIONS

C.M.E. and J.L.W. contributed to the experimental procedures and analysis. C.M.E., J.L.W., D.S., C.L.P., and L.H.T. contributed to the conception and design of the study. L.H.T. and C.M.E. wrote the manuscript. L.H.T. sourced funding for the work. All authors contributed to the manuscript revision, and read and approved the submitted version.

DECLARATION OF INTERESTS

The authors declare no competing interests.

Received: February 16, 2020

Revised: April 27, 2020

Accepted: May 13, 2020

Published: June 26, 2020

REFERENCES

- Aimone, J.B., Li, Y., Lee, S.W., Clemenson, G.D., Deng, W., and Gage, F.H. (2014). Regulation and function of adult neurogenesis: from genes to cognition. *Physiol. Rev.* *94*, 991–1026.
- Alvarez-Buylla, A., and Garcia-Verdugo, J.M. (2002). Neurogenesis in adult subventricular zone. *J. Neurosci.* *22*, 629–634.
- Amat, J.A., Ishiguro, H., Nakamura, K., and Norton, W.T. (1996). Phenotypic diversity and kinetics of proliferating microglia and astrocytes following cortical stab wounds. *Glia* *16*, 368–382.
- Arvidsson, A., Collin, T., Kirik, D., Kokaia, Z., and Lindvall, O. (2002). Neuronal replacement from endogenous precursors in the adult brain after stroke. *Nat. Med.* *8*, 963–970.
- Cavanagh, J.B. (1970). The proliferation of astrocytes around a needle wound in the rat brain. *J. Anat.* *106*, 471–487.
- Chen, X.H., Iwata, A., Nonaka, M., Browne, K.D., and Smith, D.H. (2003). Neurogenesis and glial proliferation persist for at least one year in the subventricular zone following brain trauma in rats. *J. Neurotrauma* *20*, 623–631.
- Collin, T., Arvidsson, A., Kokaia, Z., and Lindvall, O. (2005). Quantitative analysis of the generation of different striatal neuronal subtypes in the adult brain following excitotoxic injury. *Exp. Neurol.* *195*, 71–80.
- De Marchis, S., Fasolo, A., and Puche, A.C. (2004). Subventricular zone-derived neuronal progenitors migrate into the subcortical forebrain of postnatal mice. *J. Comp. Neurol.* *476*, 290–300.
- Deacon, T.W., Pakzaban, P., and Isacson, O. (1994). The lateral ganglionic eminence is the origin of cells committed to striatal phenotypes: neural transplantation and developmental evidence. *Brain Res.* *668*, 211–219.
- Ermine, C.E., Somaa, F.A., Wang, T.Y., Kagan, B.J., Parish, C.L., and Thompson, L.H. (2019). Long-term motor deficit and diffuse cortical atrophy following focal cortical ischemia in athymic rats. *Front. Cell. Neurosci.* *13*, 552.
- Frielingsdorf, H., Schwarz, K., Brundin, P., and Mohapel, P. (2004). No evidence for new dopaminergic neurons in the adult mammalian

substantia nigra. *Proc. Natl. Acad. Sci. U S A* 101, 10177–10182.

Gilmour, G., Iversen, S.D., O'Neill, M.F., and Bannerman, D.M. (2004). The effects of intracortical endothelin-1 injections on skilled forelimb use: implications for modelling recovery of function after stroke. *Behav. Brain Res.* 150, 171–183.

Inta, D., Alfonso, J., von Engelhardt, J., Kreuzberg, M.M., Meyer, A.H., van Hooft, J.A., and Monyer, H. (2008). Neurogenesis and widespread forebrain migration of distinct GABAergic neurons from the postnatal subventricular zone. *Proc. Natl. Acad. Sci. U S A* 105, 20994–20999.

Irvin, D.K., Kirik, D., Bjorklund, A., and Thompson, L.H. (2008). In vivo gene delivery to proliferating cells in the striatum generated in response to a 6-hydroxydopamine lesion of the nigro-striatal dopamine pathway. *Neurobiol. Dis.* 30, 343–352.

Li, H., and Chen, G. (2016). In vivo reprogramming for CNS repair: regenerating neurons from endogenous glial cells. *Neuron* 91, 728–738.

Liu, F., You, Y., Li, X., Ma, T., Nie, Y., Wei, B., Li, T., Lin, H., and Yang, Z. (2009). Brain injury does not alter the intrinsic differentiation potential of adult neuroblasts. *J. Neurosci.* 29, 5075–5087.

Lucassen, P.J., Fitzsimons, C.P., Salta, E., and Maletic-Savatic, M. (2019). Adult neurogenesis, human after all (again): classic, optimized, and future approaches. *Behav. Brain Res.* 381, 112458.

Luskin, M.B. (1993). Restricted proliferation and migration of postnatally generated neurons derived from the forebrain subventricular zone. *Neuron* 11, 173–189.

Marlier, Q., Verteneuil, S., Vandebosch, R., and Malgrange, B. (2015). Mechanisms and functional significance of stroke-induced neurogenesis. *Front Neurosci.* 9, 458.

Marty, S., Dusart, I., and Peschanski, M. (1991). Glial changes following an excitotoxic lesion in the CNS—I. Microglia/macrophages. *Neuroscience* 45, 529–539.

Nait-Oumesmar, B., Decker, L., Lachapelle, F., Avellana-Adalid, V., Bachelin, C., and Baron-Van Evercooren, A. (1999). Progenitor cells of the adult mouse subventricular zone proliferate, migrate and differentiate into oligodendrocytes after demyelination. *Eur. J. Neurosci.* 11, 4357–4366.

Nakatomi, H., Kuriu, T., Okabe, S., Yamamoto, S., Hatano, O., Kawahara, N., Tamura, A., Kirino, T., and Nakafuku, M. (2002). Regeneration of hippocampal pyramidal neurons after ischemic brain injury by recruitment of endogenous neural progenitors. *Cell* 110, 429–441.

Olsson, M., Campbell, K., Victorin, K., and Bjorklund, A. (1995). Projection neurons in fetal striatal transplants are predominantly derived from the lateral ganglionic eminence. *Neuroscience* 69, 1169–1182.

Parent, J.M., Vexler, Z.S., Gong, C., Derugin, N., and Ferriero, D.M. (2002). Rat forebrain neurogenesis and striatal neuron replacement after focal stroke. *Ann. Neurol.* 52, 802–813.

Plane, J., Whitney, J., Schallert, T., and Parent, J. (2008). Retinoic acid and environmental enrichment alter subventricular zone and striatal neurogenesis after stroke. *Exp. Neurol.* 214, 125–134.

Sanai, N., Nguyen, T., Ihrie, R.A., Mirzadeh, Z., Tsai, H.H., Wong, M., Gupta, N., Berger, M.S., Huang, E., Garcia-Verdugo, J.M., et al. (2011). Corridors of migrating neurons in the human brain and their decline during infancy. *Nature* 478, 382–386.

Somaa, F.A., Wang, T.Y., Niclis, J.C., Bruggeman, K.F., Kauhausen, J.A., Guo, H., McDougall, S., Williams, R.J., Nisbet, D.R., Thompson, L.H., and

Parish, C.L. (2017). Peptide-based scaffolds support human cortical progenitor graft integration to reduce atrophy and promote functional repair in a model of stroke. *Cell Rep.* 20, 1964–1977.

Teramoto, T., Qiu, J., Plumier, J.C., and Moskowitz, M. (2003). EGF amplifies the replacement of parvalbumin-expressing striatal interneurons after ischemia. *J. Clin. Invest.* 111, 1125–1132.

van der Kooy, D., and Fishell, G. (1987). Neuronal birthdate underlies the development of striatal compartments. *Brain Res.* 401, 155–161.

Wright, J., Stanic, D., and Thompson, L.H. (2013). Generation of striatal projection neurons extends into the neonatal period in the rat brain. *J. Physiol.* 591, 67–76.

Wright, J.L., Chu, H.X., Kagan, B.J., Ermine, C.M., Kauhausen, J.A., Parish, C.L., Sobey, C.G., and Thompson, L.H. (2018). Local injection of endothelin-1 in the early neonatal rat brain models ischemic damage associated with motor impairment and diffuse loss in brain volume. *Neuroscience* 393, 110–122.

Wright, J.L., Ermine, C.M., Jorgensen, J.R., Parish, C.L., and Thompson, L.H. (2016). Over-expression of meteorin drives gliogenesis following striatal injury. *Front. Cell. Neurosci.* 10, 177.

Yang, Z., You, Y., and Levison, S.W. (2008). Neonatal hypoxic/ischemic brain injury induces production of calretinin-expressing interneurons in the striatum. *J. Comp. Neurol.* 511, 19–33.

Zhao, M., Momma, S., Delfani, K., Carlen, M., Cassidy, R.M., Johansson, C.B., Brismar, H., Shupliakov, O., Frisen, J., and Janson, A.M. (2003). Evidence for neurogenesis in the adult mammalian substantia nigra. *Proc. Natl. Acad. Sci. U S A* 100, 7925–7930.

iScience, Volume 26

Supplemental Information

Ischemic Injury Does Not Stimulate Striatal Neuron Replacement Even during Periods of Active Striatal Neurogenesis

Charlotte M. Ermine, Jordan L. Wright, Davor Stanic, Clare L. Parish, and Lachlan H. Thompson

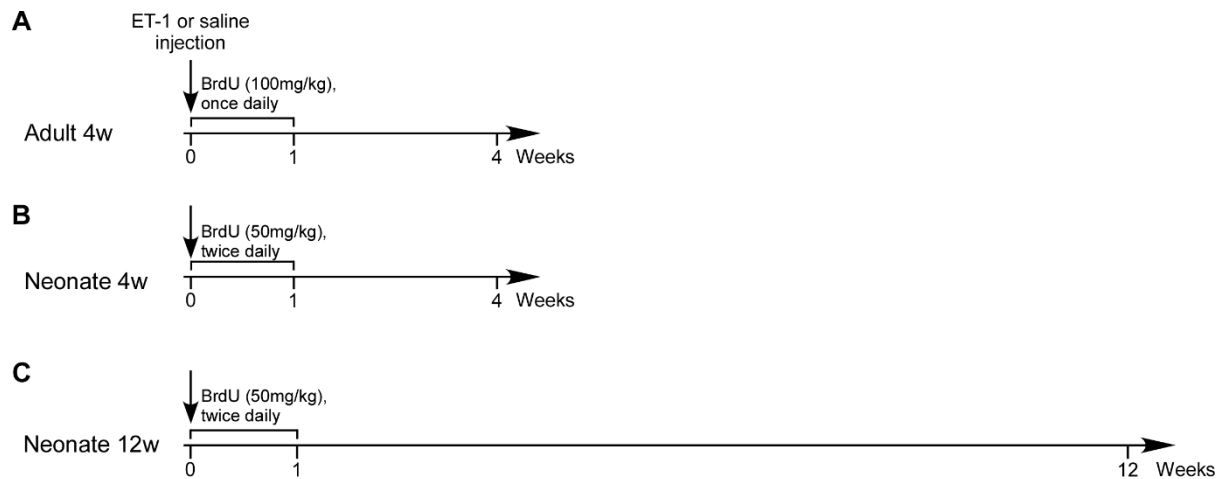


Figure S1: Experimental design: (A) related to figure 1 and 2, (B) related to figure 3 and 4 and (C) related to figure 5 and 6. At day zero all groups underwent stereotaxic surgery for injection of ET-1 or saline into the striatum. One day after surgery, all animals were injected intraperitoneally with 5-bromo-2'-deoxyuridine (BrdU) for seven days, once daily at 100mg/kg for the adult groups (A) and twice daily at 50mg/kg for the neonatal group (B-C). The animals were taken for histological analysis at four weeks (A-B) or twelve weeks after surgery (C).

Transparent Methods

Animals and Experimental Design

Adult, female Sprague Dawley or neonatal (postnatal day 1; P1), mixed-sex Sprague Dawley rats were used in this study. All animals were housed in individually ventilated cages under a 12h light/dark cycle with *ad libitum* access to food and water. The use of animals in this study conformed to the Australian National Health and Medical Research Council's published Code of Practice for the Use of Animals in Research and were approved by the Florey Institute of Neuroscience and Mental Health animal ethics committee. In our initial investigations, we explored the phenotypic fate of newborn cells four weeks after ischemic injury to the adult (Adult 4W) or neonatal (Neonate 4W) striatum. To assess longer-term survival and allow further time for acquisition of mature markers of phenotypic identity, we also characterised the fate of newborn cells twelve weeks following initial birth-dating after neonatal ischemic injury (Neonate 12W). The experimental timeline is represented in Supplementary Figure S1.

Stereotaxic surgery

Striatal ischemia was induced by injection of ET-1 (800 pMol in 1 μ l) to the anterior head of the striatum. Stereotaxic co-ordinates: adults - 0.5 mm rostral, 3.0 mm lateral to bregma and 5.0 mm below the dural surface; neonates - 0.7 mm rostral, 2.3 mm lateral to bregma and 2.9 mm below dura. Controls received the same volume of sterile saline (0.9%). Adult animals were anaesthetised with isoflurane (induction at 5% and maintenance at 2% at 1L/min) and placed in a stereotaxic frame (Kopf, Germany). The neonatal rats were anaesthetised through

hypothermia, induced by placing the pup in ice. The neonatal animals were placed in a Cunningham adaptor stage (Stoelting, Germany) fitted to the stereotaxic frame and anaesthesia was maintained with dry ice added to absolute ethanol held in the reservoir of the Cunningham adaptor. The animals were perfused for histology at either four- or twelve-weeks post-surgery.

BrdU treatment

Birth-dating of cells over the first week after saline or ET-1 injection was performed through administration of the thymidine analogue 5-bromo-2'-deoxyuridine (BrdU), which is incorporated in dividing cells during DNA synthesis. One day after surgery, BrdU (20mg/ml in 0.9% saline) was injected intraperitoneally (i.p.) at a dose of 100mg/kg once a day for seven days for the adult group and at 50mg/kg, twice daily for seven days for the neonatal groups (Supp. Figure 1). The dosage was the same between the adult and neonatal groups, however the regime was adapted for each group, to allow for injection volumes in the smaller animals.

Tissue collection and immunohistochemistry

Following a terminal dose of pentobarbitone (100mg/kg; Virbac, Peakhurst, Australia) animals were transcardially perfused with 50ml 0.2M phosphate buffered saline and 250ml paraformaldehyde (PFA, 4% in 0.2M phosphate buffer with 0.2% picric acid). The brains were collected and post-fixed in PFA for 2 hours, followed by cryo-protection in 20% sucrose PBS solution for one to two days. The brains were snap frozen on dry ice and coronal sections were collected in series at 40 μ m using a freezing-microtome (Leica, Wetzlar, Germany).

Free-floating immunohistochemistry was performed on a 1:12 series for chromogenic labelling of BrdU or combined fluorescent labelling of BrdU, NeuN, Darpp32 and Calretinin (CR), as previously described in (Wright et al., 2013). Tissue labelled for BrdU was pre-treated by incubation in deionized formamide (Merck Millipore) at 65°C for 2 hours, followed by 2M HCL at 27°C for 30 minutes and washes in Borate buffer at room temperature for 20 minutes. Primary antibodies and dilutions used were: sheep anti-BrdU (Exalpha, A205P, 1:1000); mouse anti-NeuN (Millipore, MAB377, 1:1000); rabbit anti-CR (SWANT # CG1, 1:4000) and rabbit anti-Darpp32 (Millipore, AB10518, 1:500). Secondary antibodies and dilutions used were: anti-sheep and anti-rabbit conjugated Dylight Fluorophores 488 and 647 (Jackson ImmunoResearch, 1:200) for fluorescent staining and anti-sheep biotin conjugated (Jackson ImmunoResearch, 1:400) for chromogenic staining. Fluorescent staining for NeuN was amplified using the secondary antibody anti-mouse biotin-conjugated and streptavidine-550 (Abcam, 134348, 1:400).

Imaging and cell counting

Fluorescent microscopic analysis and images were performed using a Zeiss Meta confocal microscope (LSM 780), chromogenic images were captured using a Leica DM6000 microscope.

For cell counting, three consecutive sections spanning the anterior head of the striatum (approximately located at +1.70 mm, +1.20 mm, +0.70 mm relative to bregma) were captured

using a 20x objective with optical slicing in the Z axis and reconstruction of each panel across the X and Y axes to produce a composite image of the entire striatal volume for each section. The number of BrdU+ cells was estimated using the spot creation module in Imaris v9.0. The total number of cells and the density in the anterior striatum (bregma +1.70 – +0.70 mm) was estimated by extrapolation according to the Cavalieri principle (Cavalieri, 1966).

To assess expression of phenotypic markers NeuN, Darpp32 or CR in BrdU+ cells, instances of co-expression were initially estimated via Imaris using the spot creation module for individual channels and subsequent processing to determine overlap. Instances of co-expression were manually verified on the X, Y and Z planes using Zen lite software. All sections were also manually inspected to identify possible false-negatives not captured by Imaris. The total frequency of each cell type was determined and density estimated using Cavalieri's principle (Cavalieri, 1966).

Statistical analysis

Statistical analysis was performed using Prism 7 (GraphPad Software). For the adult group we used Welch's *t* test for: lesion volume, BrdU, BrdU/NeuN, BrdU/NeuN/CR absolute numbers and densities; and we used unpaired *t* test for: BrdU/CR density and absolute number. For the neonatal four-weeks group we used unpaired *t* test for: BrdU cell number and density, BrdU/NeuN density, BrdU/NeuN/Darpp32 cell number, BrdU/CR density, BrdU/NeuN/CR cell number; and Welch's *t* test for BrdU/NeuN cell number, BrdU/NeuN/Darpp32 density, BrdU/CR cell number and BrdU/NeuN/CR density. For the neonatal twelve-weeks group, we used unpaired *t* test for BrdU, BrdU/NeuN, BrdU/NeuN/Darpp32 cell number and densities, and BrdU/CR and BrdU/NeuN/CR cell number; and Welch's *t* test for: BrdU/CR and BrdU/NeuN/CR densities.

Supplemental References

WRIGHT, J., STANIC, D. & THOMPSON, L. H. 2013. Generation of striatal projection neurons extends into the neonatal period in the rat brain. *J Physiol*, 591, 67-76.